Accepted Manuscript

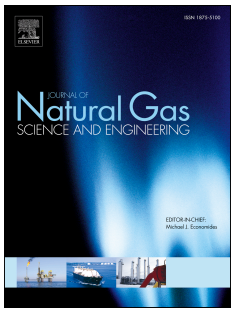

Influence of coupled effect among flaw parameters on strength characteristic of precracked specimen: Application of response surface methodology and fractal method

Ting Liu, Baiquan Lin, Chunshan Zheng, Quanle Zou, Chuanjie Zhu, Fazhi Yan

PII: S1875-5100(15)30042-1

DOI: 10.1016/j.jngse.2015.07.021

Reference: JNGSE 879

To appear in: *Journal of Natural Gas Science and Engineering*

Received Date: 17 April 2015

Revised Date: 12 July 2015

Accepted Date: 13 July 2015

Please cite this article as: Liu, T., Lin, B., Zheng, C., Zou, Q., Zhu, C., Yan, F., Influence of coupled effect among flaw parameters on strength characteristic of precracked specimen: Application of response surface methodology and fractal method, *Journal of Natural Gas Science & Engineering* (2015), doi: 10.1016/j.jngse.2015.07.021.

This is a PDF file of an unedited manuscript that has been accepted for publication. As a service to our customers we are providing this early version of the manuscript. The manuscript will undergo copyediting, typesetting, and review of the resulting proof before it is published in its final form. Please note that during the production process errors may be discovered which could affect the content, and all legal disclaimers that apply to the journal pertain.

ACCEPTED MANUSCRIPT

*Corresponding author: Baiquan Lin
E-mail: lbq21405@126.com
Tel: +8618361237581

Influence of coupled effect among flaw parameters on strength characteristic of precracked specimen: Application of response surface methodology and fractal method

Ting Liu[a, b], Baiquan Lin[a, b*], Chunshan Zheng[c], Quanle Zou[a, b], Chuanjie Zhu[a, b], Fazhi Yan[a, b]

[a] *School of Safety Engineering, China University of Mining & Technology, Xuzhou, PRC 221116*

[b] *State Key Laboratory of Coal Resources and Safe Mining, Xuzhou, PRC 221116*

[c] *School of Mechanical and Mining Engineering, the University of Queensland, QLD 4072, Australia*

Abstract: Hydraulic slotting is an effective method for enhanced coalbed methane (ECBM) recovery, and it has been widely employed in China. Although there have been many studies of this technique, the influence of slot parameters on the strength characteristic of the coal, which is an important factor that affects the permeability enhancement effect, has rarely been studied. Thus, only limited information is available regarding the pressure relief and permeability enhancement mechanisms of this technique. In the current study, the influence of flaw parameters on the compressive strength of a precracked sample under biaxial compression is discussed. The results indicate that an increase in the flaw length and width has a negative effect on the compressive strength, whereas an increase in the flaw inclination angle has a positive effect on the compressive strength. The results of the response surface methodology (RSM) indicate that the interactions among the flaw parameters have a significant influence on the compressive strength. The propagation patterns of cracks are quantified by the fractal dimension, which is used to explore the mechanism of compressive strength variation with changes in the flaw parameters. The study results indicate that the variation in the flaw parameters changes the propagation pattern of cracks, resulting in different compressive strengths. In addition, an opposite variation trend of the compressive strength and fractal dimension with flaw parameters is also observed. The research results are expected to guide the field application of hydraulic slotting.

Keywords: Compressive strength; Hydraulic slotting; Flaw parameters; RSM; Fractal dimension

1. Introduction

Gas disasters in coalmines typically involve the explosion of gas and coal and gas outbursts, which are major threats to miner safety and to the property of the coal mine enterprise during coal exploration (Liu et al, 2014; Yang et al, 2009; Zhang et al., 2015; Zhou et al., 2014; Zhou et al., 2015; Wang et al., 2012; Hungerford et al., 2013; Chen et al., 2014; Xia et al., 2014). In addition, coalbed methane (CBM) is a type of fuel that is characterized by its high calorific value and low environmental impact, i.e., clean energy (Zou et al., 2014a, 2014b; Ni et al., 2014). Moreover, CH_4, the primary component of CBM, is a greenhouse gas that has a greenhouse effect 21 times greater

than that of CO_2 (Wang and Cheng, 2012; Cheng et al., 2011; Wang et al., 2012; Zhang et al., 2014). Therefore, proper management of coal-mine gas can have a threefold effect, namely, mining safety, energy utilization, and environment protection. Gas drainage, which is an interesting topic worldwide, can eliminate the risk of a gas explosion, provide a clean energy resource, and aid in environmental protection (Xia et al., 2014). However, the coal seams in China are characterized by numerous micropores, low permeability, strong adsorption, and high gas pressure (Ni et al., 2014). The permeability of the coal seams in most Chinese mines ranges from 10^{-4} to 10^{-3} mD, which is three to four orders of magnitude lower than those in Australia and the United States (Xia et al., 2014; Wang et al., 2012; Meng et al., 2015). Therefore, to improve the gas–drainage efficiency, measures to relieve the pressure and enhance the permeability should be taken to improve the permeability of the coal seam.

Hydraulic slotting, which is based on high-pressure water-jet technology, has been accepted as an effective and reliable technique to artificially enhance the permeability. This technique has been widely used in many coal mines in China to improve the gas drainage efficiency (Yan et al., 2015; Lin et al., 2014, 2015; Lu et al., 2009, 2011; Zou et al., 2014a, 2014b; Shen et al., 2014, 2012a, 2012b). Fig.1 shows the hydraulic slotting system and the slotting process. The arrows in Fig.1(a) show the direction of water flow. When water flows out of the dual-power drill bit, a high-pressure waterjet is formed which creates flaws on the surface of coal. The area thus formed is termed the “pressure relief space”. Under the influence of stress, fractures, which are the potential migration pathways for gas, are initiated, and they propagate gradually around the flaws [see Fig. 1 (b)].

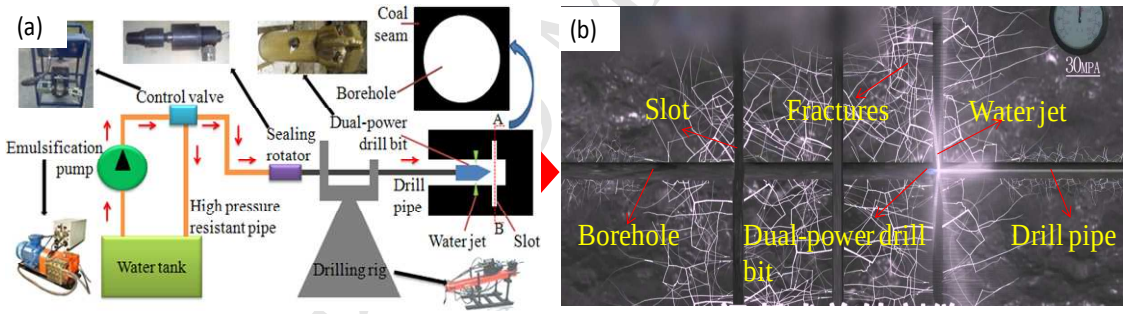

Fig. 1. Constitution of the hydraulic slotting system and its operation process. a. The hydraulic slotting system and its components; b. the waterjet slotting process and a sketch of the flaw.

The application of this technique has advanced the simultaneous exploitation of coal and gas, which is an essential component of China’s current energy structure (Wang and Cheng, 2012). Due to the importance of this technology, many studies have been conducted on hydraulic slotting to elucidate the mechanisms by which it relieves pressure and enhances permeability. Lu et al. (2010) conducted a study on high-pressure pulsed water jet based on a rock damage constitutive model. The results indicated that the impact and vibration effects of the pulsed water jet could effectively crush coal, improve the connectivity of fractures and the permeability of the coal mass. Yan et al. (2015) presented a novel ECBM extraction technique, which was a combination of hydraulic slotting and hydraulic fracturing. Their field test results showed that the amount of CBM extracted using this technique was 8.75 times greater than that extracted from ordinary drilling. Shen et al. (2014, 2012a, 2012b) investigated the displacement, stress distribution, and seepage characteristics around a slotted borehole using *FLAC*^{3D} software. These researchers also analyzed the mechanism used by hydraulic slotting to relieve pressure and enhance permeability. Lin et al.

(2015, 2014) numerically analyzed the crack propagation patterns, stress, porosity, and energy evolution rules around a slotted borehole using PFC^{2D} software. These researchers' study results showed that the existence of a flaw is favorable for the propagation of cracks and an increase in coal porosity, both of which improve the gas drainage efficiency. Zou et al. (2014a, 2014b) investigated the variations in the pore structure of coal after hydraulic slotting and gas drainage. Based on the analysis, the gas adsorption properties of coal around a slotted borehole were also discussed. Lu et al. (2009, 2011) experimentally and numerically investigated the application of the water-jet technique on gas drainage and the prevention of outbursts during gate road development. The recorded data showed that the methane drainage efficiency achieved by this method was three to six times higher than traditional methods and the values of S_{max} and K_1, which are determined by drill cuttings and describe the possibility that an outburst will occur, were maintained below the critical limit of 70%.

These aforementioned studies indicate that the research to date has primarily investigated the impact properties, the rock-breaking characteristics of waterjets, and the seepage behavior, pore structure, and adsorption property of coal after hydraulic slotting. However, little attention has been paid to the influence of slot parameters on the strength of the coal, which is an important factor affecting the increase in permeability.

Recently, extensive research has been conducted on the mechanical characterization of rock-like specimens with pre-existing flaws, and some valuable findings have been published. Based on the research method applied, the results can be divided into the three parts, i.e., theoretical analyses, physical experiments and numerical simulations (Liu et al., 2015). In the theoretical analyses, Yuan et al. (2013) proposed a micromechanical elastoplastic damage model for rock-like materials under compression based on the growth of pre-existing flaws. The numerical calculation was performed to investigate the effects of the friction coefficient and the initial flaw size on the compressive strength and damage evolution. Zhou et al. (2010) presented a microcrack damage model for brittle rocks under uniaxial compression based on a supposed random distribution of microcracks. Laboratory test results were used to verify the practicability of the model. Paliwal and Ramesh (2008) developed a brittle failure model for rocks under compression that considered the interactions of microcracks. The influence of the flaw size was discussed in the numerical simulation. In the aspect of the laboratory experiments, Wong and Chau (1998) experimentally studied the influences of the inclination angle, bridge angle, and coefficient of friction on the crack coalescence pattern and the strength of a sandstone-like material containing two parallel inclined flaws under uniaxial compression. Three crack coalescence modes, namely, the shear mode, the mixed shear/tensile mode, and the wing tensile mode, were observed. Yang et al. (2008, 2009) investigated the strength and failure behavior of precracked marble under uniaxial and triaxial compression. The results showed that the compressive strength of a precracked sample was closely related to the geometry of the flaw. Lee and Jeon (2011) studied the crack initiation, propagation, and coalescence near the pre-existing flaw. The variation in the compressive strength of the precracked sample based on the flaw inclination angle was also investigated. Park and Bobet (2009) conducted extensive experiments on gypsum specimens under uniaxial compression with closed and open flaws and made a comparison between these two specimens. Wong and Einstein (2009) investigated crack propagation in molded gypsum and Carrara marble with a single flaw and identified seven crack types based on the geometry and propagation mechanism. In the numerical simulations, specimens

with a single flaw and two parallel flaws were investigated under uniaxial compression by Zhang and Wong (2012, 2013a) using PFC^{2D} software. The processes of crack initiation, propagation, and coalescence were analyzed, while the stress and displacement distributions around the flaw were also studied. Manouchehrian et al. (2014) monitored the crack propagation processes of precracked specimens with different flaw orientations under uniaxial and biaxial compression using PFC^{2D} software. Li and Wong (2012) analyzed the influence of the flaw inclination angle on the cracking processes using the finite element method (*FEM*) and the nonlinear dynamics method. The results showed that the analysis of the stress field resulted from the existence of the flaw provides a better understanding of the influence of the flaw inclination angle on the initiation position and initiation angle of potential cracks.

The analysis shows that the research to date has primarily examined the influence of a single factor of flaws on mechanical properties, while few studies investigating the influence of the coupled effect of flaw parameters on the strength and the quantitative relationship between the crack propagation patterns and the compressive strength of the precracked specimen have been published.

Based on these analyses, a numerical model is established using PFC^{2D} software to investigate the influence of the flaw parameters on the compressive strength of the specimen with a single pre-existing flaw. The research results are expected to provide guidance to the field application of hydraulic slotting.

In this work, the influence of the coupling effect of flaw parameters on the strength of the precracked specimen is studied using the response surface methodology and the fractal method. First, the influence of a single flaw parameter on the compressive strength is discussed in Section3.1. Then, the influence of the coupled effect of flaw parameters is investigated in Section 3.2 using the response surface methodology. Next, the relationship between the fractal dimension of crack propagation patterns and the compressive strength is reported in Section 4. Finally, the conclusions are presented in Section 5.

2. Modeling

A numerical model with the following dimensions was constructed: height, 120 mm and width, 60 mm (Fig.2). In the figure, l, w and θ are the length, width and inclination angle of the flaw, respectively. The numerical model contained approximately 30,000 particles, which were determined with regard to the computing power and the representativeness of the calculation results. The particle size followed a uniform distribution ranging from 0.2 mm to 0.3 mm. Table 1 lists the more comprehensive parameters of the model, which were mainly obtained from those presented by Wang (2014), with some appropriate changes. A single flaw was created at the center of the specimen by deleting particles in the designated area. The geometric parameters of the flaw were set according to field operation data of hydraulic slotting. During hydraulic slotting, the maximum length of a flaw can reach up to 0.4 m, which corresponds to the maximum flaw length of 20 mm in the model. For the flaw width, the dimension can be adjusted during field hydraulic slotting by pulling the drill pipe. The maximum width of the flaw was determined to be 0.12 m, which corresponds to the maximum flaw width of 6 mm in the model. Thus, the similarity ratio of the numerical model to the actual model is 20. The flaw inclination angle can be changed from 0° to 90° by rotating the drill pipe. In this paper, the length of the flaw varies from 10 to 20 mm at 2 mm intervals; the width varies from 1 to 6 mm at 1 mm intervals; and the inclination angle varies

from 0 to 90° at 15° intervals.

Because of the heterogeneity and randomness introduced in *PFC* with regard to the microstrength and particle radius, no two *PFC* runs produce the same results. This characteristic allows for a more realistic simulation of the natural coal-rock mass (Cho et al., 2007; Zhang and Wong, 2012).

The numerical model was loaded vertically in a constant displacement-control manner, while the horizontal direction was subjected to a constant confining pressure (5 MPa). To ensure that the specimen remained in a quasistatic equilibrium during the test, a sufficiently low loading rate of 0.02 m/s was applied. According to Zhang and Wong (2013b), this loading rate is reasonable for performing an analysis under static load using the bonded particle model.

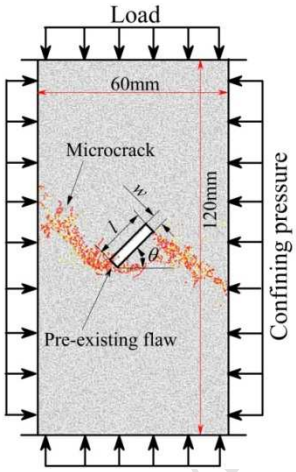

Fig.2. Schematic plane view of the precracked specimen (height, 120 mm; width, 60 mm) with a single flaw created at the center.

Table 1

Mesoscopic mechanical parameters of coal mass

Particle density ρ_C /kgm^{-3}	Friction coefficient μ	Contact modulus E_C /GPa	Parallel-bond modulus E_P /GPa	Normal strength σ_C /MPa		Shear strength τ_C /MPa		Ball stiffness ratio k_n / k_s	Parallel-bond stiffness ratio $\overline{k_n} / \overline{k_s}$
				Mean value	Standard deviation	Mean value	Standard deviation		
1635.0	0.7	2.4	2.4	7.0	0.1	7.0	0.1	1.0	1.0

3. Strength characteristics of the precracked specimen

First, to investigate the influence of a flaw on the strength properties of a precracked specimen systematically, the effects of flaw length, width, and inclination angle on the sample strength were studied. Then, the coupled effects of the three factors were studied. Because the same calculation result cannot be achieved by any two *PFC* runs due to the heterogeneity and randomness introduced in *PFC* (Cho et al., 2007; Zhang and Wong, 2012), all numerical models used in this work were calculated three times to make the results more representative and reliable, unless otherwise stated. The final result is the average value of the three calculated values.

3.1. Influence of a single flaw parameter on the strength of the precracked specimen

(1) Flaw length

To explore the relationship between flaw length and strength behavior, the control variate method was adopted, and the flaw width and inclination angle were fixed at 3 mm and 45°, respectively.

As depicted in Fig.3, the compressive strength of the precracked specimen decreases with an increase in the flaw length. When l<16 mm, the compressive strength shows a sharp decrease with an increase in the flaw length. When l increases from 10 mm to 16 mm, the compressive strength decreases by 12.04%, which means that if l increases by 1 mm, the compressive strength will decrease by 2%. When 16<l<18 mm, the compressive strength shows little change. When l increases from 18 to 20 mm, the compressive strength decreases by 6.06%. The aforementioned analysis implies that the compressive strength exhibits strong nonlinear variation with the flaw length.

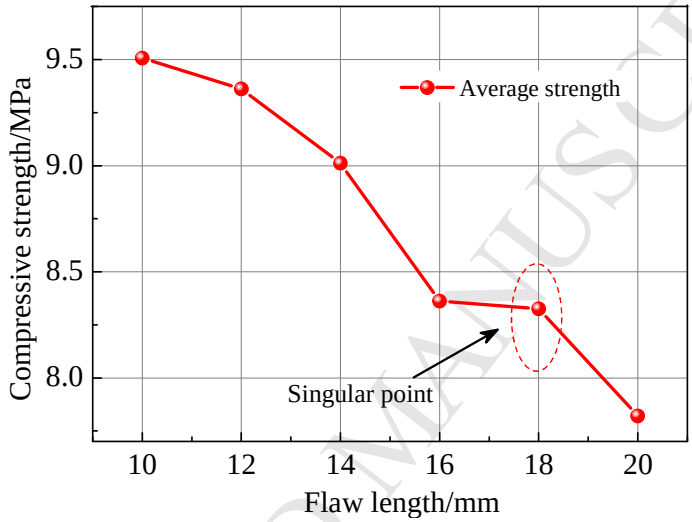

Fig.3. Relationship between the flaw length and the compressive strength of the precracked specimen.

(2) Flaw width

To investigate the variation of the compressive strength with flaw width, the flaw length and inclination angle were kept constant, with values of 16 mm and 45°, respectively.

Fig.4 shows the relationship between the compressive strength and the flaw width. With an increase in the flaw width, the average value of compressive strength decreases gradually, except at the point corresponding to w=5 mm. In addition, the variation trend flattens out gradually.

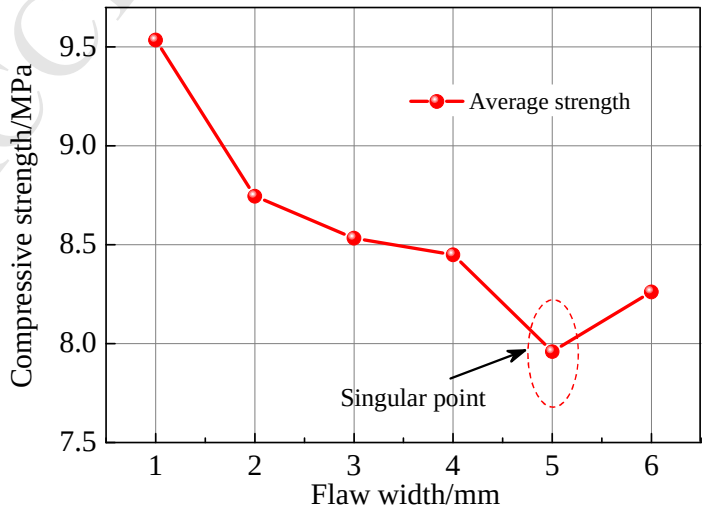

ACCEPTED MANUSCRIPT

Fig.4. Relationship between the flaw width and the compressive strength of the precracked specimen.

(3) Flaw inclination angle

For the analysis of the relationship between the flaw inclination angle and the compressive strength of the precracked specimen, the flaw length and width were kept constant, with values of 16 mm and 3 mm, respectively.

Fig.5 shows the variation of the compressive strength with the flaw inclination angle. The compressive strength displays an increasing trend with an increase in the flaw inclination angle on the whole, except at the points related to θ=15° and 75°.

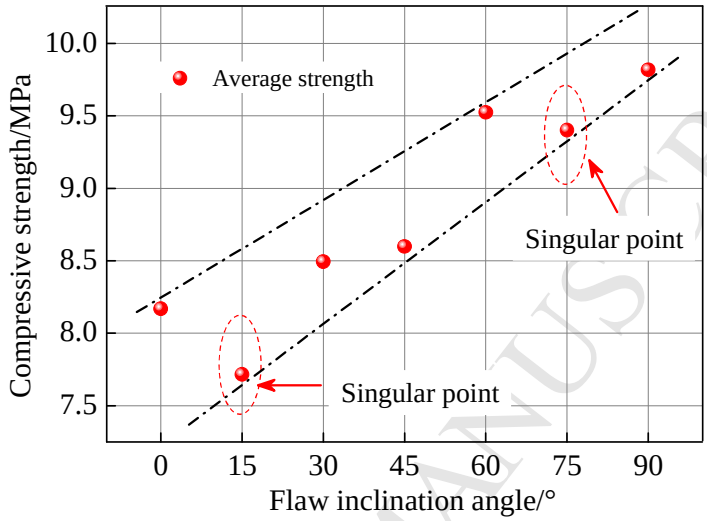

Fig.5. Relationship between the flaw inclination angle and the compressive strength of the precracked specimen.

3.2. Influence of the coupled effects of flaw parameters on the strength of the precracked specimen

From Figs.3–5, we can find that the variations in the compressive strength with the length, width, and inclination angle of the flaw all show nonlinearity. Thus, it can be deduced that some other factors must exist that affect the variation trend of the compressive strength. However, because the control variate method was adopted in the aforementioned analysis, we infer that coupled effects must exist among the three factors considered. Therefore, to further understand the relationship between the compressive strength and the flaw parameters, it is necessary to identify the way in which the coupled effects of the flaws influence the compressive strength.

The major disadvantages of the control variate method used are as follows: (1) a large number of experiments are needed, which increases both the necessary time and resources; and (2) the probable interactions between the independent variables are not considered. To avoid these problems, the response surface methodology was adopted in our research (Sodeifian et al., 2014).

3.2.1 Response surface methodology

Response surface methodology (RSM), a collection of mathematical and statistical techniques, has been found to be a functional aid in exploring the interactions of multiple factors on the response of a system (Kirmizakis et al., 2014; Sodeifian et al., 2014; Yuan et al., 2015). During an analysis, it is very important to select an appropriate method that can evaluate the influence of independent variables and their coupled effects on the dependent variable with fewer experiments. RSM provides a great deal of information with only a small number of tests to monitor the interactions among variables on the response (Sodeifian et al., 2014; Kirmizakis et al.,

2014).

In this study, the mathematical modeling was conducted using the *Design-Expert 8.0.5b* software. The central composite design (CCD) module was used to model RSM. The independent variables (the influencing factors of the compressive strength) contained in the modeling process are the flaw length, width, and inclination angle, which are coded as x_1, x_2, x_3, respectively. The dependent variable is the compressive strength of the precracked specimen, which can be expressed using a quadratic model as follows: (Noshadi et al., 2012; Kirmizakis et al., 2014;Yuan et al., 2015).

$$R = \sum_{i=1}^{3} \beta_{ii} X_i^2 + \sum_{i=1}^{3} \sum_{j=i+1}^{3} \beta_{ij} X_i X_j + \sum_{i=1}^{3} \beta_i X_i + \beta_0 \tag{3}$$

where R is the response variable representing the compressive strength of the precracked specimen; β_{ii}, β_{ij}, β_i, and β_0 are regression coefficients; and X_i and X_j are the values of the independent variables coded in the program and can be expressed as follows:

$$X_i = \frac{x_i - x_0}{\Delta x} \tag{4}$$

where x_0 is the value of x_i at the center point and Δx is the change step.

The code and level of the independent variables in the CCD are shown in Table 2. A total CCD experiment contains 20 points. Among them, 15 points are factorial points and 5 points are zero points which are used to estimate the experimental error. The CCD experiment scheme and results are presented in Table 3. Note that the experimental result is the compressive strength obtained by the numerical test and the predicted result represents the compressive strength calculated by RSM.

Table 2

Independent variable code and level in the CCD experiment.

Factor	Code	Level		
		-1	0	1
Flaw length/mm	X_1	12	16	20
Flaw width/mm	X_2	2	4	6
Flaw inclination angle/°	X_3	20	45	70

Table 3

CCD experiments and the experimental results.

Experiment number	Experiment design			Experimental result/MPa	Predicted result/MPa
	Flaw length/mm	Flaw width/mm	Flaw inclination angle/°		
1	0	0	0	8.61	8.51
2	1	1	1	8.60	8.51
3	0	0	0	8.61	8.51
4	0	0	0	8.61	9.18
5	0	0	0	7.40	7.50
6	1	-1	1	8.61	8.51
7	1	-1	-1	7.51	7.12

8	1	1	-1	10.44	10.48
9	1.682	0	0	7.17	6.79
10	-1.682	0	0	9.32	9.23
11	0	-1.682	0	8.29	8.50
12	0	1.682	0	9.76	9.46
13	0	0	1.682	8.27	8.47
14	0	0	-1.682	8.62	8.51
15	0	0	0	8.61	7.32
16	-1	-1	-1	7.93	7.32
17	0	0	0	8.61	8.51
18	-1	1	-1	9.51	9.19
19	-1	-1	1	6.06	6.52
20	-1	1	1	7.07	7.37

3.2.2 Analysis of variance (ANOVA)

To determine whether the quadratic model obtained to explain the experiment data at a 95% confidence interval is statistically significant, we tested the model using an analysis of variance (ANOVA) (Kirmizakis et al., 2014). An F value of 11.08 was obtained from the ANOVA, which indicates that the model is significant and there is only a 0.04% chance that a "model *F* value" this large could occur due to noise. In addition, the "Adeq Precision" measures the signal-to-noise ratio. A ratio greater than 4 is desirable. The ratio of 12.775 indicates an adequate signal, which means that this model can be used to navigate the design space. The "lack-of-fit *F* value" of 3.55 implies that there is a 9.52% (<10%) chance that a "lack-of-fit *F* value" this large could occur due to noise. Lack of fit is not significant. The fit accuracy of the model is mainly controlled by the coefficient of determination (R^2). According to the ANOVA results, the R^2 of the model is 0.9088, indicating a great correlation between the experimental value and the predicted value. In addition, the actual and predicted compressive strength depicted in Fig.6 shows a linear regression relationship, which also verifies the conclusion drawn above. The relationship between the normal percentage probability and the studentized residual is depicted in Fig.7. A nonlinear pattern (an "S-shaped curve") indicates non-normality in the error term. In Fig. 7, a linear dependence is observed, meaning that a response transformation is not needed, nor is there any obvious problem with the normality.

All these aforementioned analyses prove that the quadratic response model is suitable for the CCD experiment and the prediction of the compressive strength.

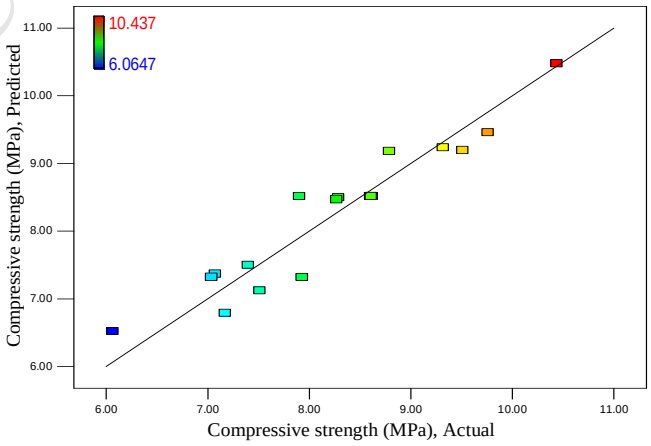

Fig.6. The actual and predicted compressive strength of the precracked specimen.

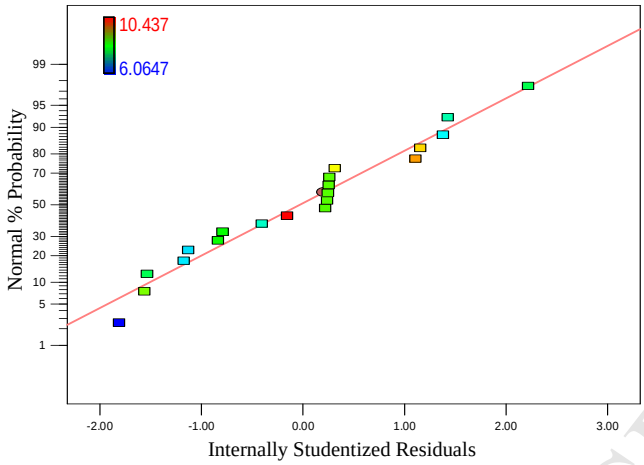

Fig.7. Normal probability plot for the compressive strength.

3.2.3 Multiple regression modeling

The polynomial model, a function of flaw length, width, and inclination angle, was obtained according to the data listed in Table 3. The final response equation can be expressed as follows:

$$R = 8.51 - 0.71X_1 - 0.57X_2 + 0.69X_3 + 0.037X_1X_2 - 0.25X_1X_3 - 0.041X_2X_3 - 0.18X_1^2 - 0.084X_2^2 - 0.08X_3^2 \quad (5)$$

where R is the response of the compressive strength, and X_1, X_2 and X_3 are the related coded variables of flaw length, flaw width, and flaw inclination angle, respectively.

3.2.4 Response surface analysis

To elucidate the influences of flaw parameters and the coupling effect on the compressive strength, 3D plots of the relationship between the dependent variable and two independent variables when the other variable is at the middle level are depicted in Fig.8.

Fig.8(a) shows the influence of the flaw length and width on the compressive strength when the flaw inclination angle is at the middle level. As seen in Fig.8(a), while the flaw width is constant, an increase in the flaw length will have a negative effect on the compressive strength. It is important to note that when *w=2* mm, an increase in the flaw length from 10 mm to 20 mm will cause a 15.03% reduction in the compressive strength (from 9.6103 MPa to 8.1657 MPa); however, when *w*=6 mm, a 19.55% reduction is caused by an increase of flaw length from 10 mm to 20 mm (8.4684 MPa to 6.8129 MPa). This finding implies that an increase in the flaw width increases the capacity of the flaw length to weaken the compressive strength. When the flaw length is constant, an increase in the flaw width causes a decrease in the compressive strength. When *l=10 mm*, if the flaw width increases from 2mm to 6 mm, the compressive strength will decrease by 11.88% (from 9.6103 MPa to 8.4684 MPa), and when *l* = 20 mm, an increase of the flaw width from 2 mm to 6 mm will lead to a 16.56% reduction in the compressive strength. This result indicates that the increase in the flaw length will also enhance the capacity of the flaw width to weaken the compressive strength.

The influence of the coupled effect between the flaw length and the inclination angle on the compressive strength is plotted in Fig.8(b). With an increase in the flaw inclination angle, the compressive strength rises gradually; however, Fig. 8(b) shows an inverse trend with an increase

of the flaw length, which agrees with the result observed in Fig.8(a). Note that when *l=10 mm*, the increase of the inclination angle from 0° to 90° will result in an increase in the compressive strength from 6.9877 MPa to 10.8378 MPa, an increase of 55.10%. Whereas when *l=20 mm* and the flaw inclination angle rises from 0 to 90°, the compressive strength will increase by 24.16% (from 6.5655 MPa to 8.1515 MPa). This difference suggests that an increase in the flaw length weakens the capability of the flaw inclination angle to enhance the compressive strength. When θ=0°, if the flaw length increases from 10 mm to 20 mm, the compressive strength will only decrease by 6.04% (from 6.9877 MPa to 6.5655 MPa), whereas when θ=90°, the compressive strength will decrease by 24.79%. This comparison shows that as the flaw inclination angle increases, the ability of the flaw length to reduce the compressive strength increases.

Fig.8(c) depicts the relationship between the flaw width, inclination angle, and the compressive strength. It can be observed that an increase in the flaw width will cause a negative effect on the compressive strength, whereas a rise in the flaw inclination angle will lead to a positive effect on the compressive strength. Analogous to the aforementioned analysis, the interaction between the flaw width and the inclination angle was also investigated. When *w=2 mm*, an increase of the inclination angle from 0 to 90° will lead to an increase of 35.63% in the compressive strength (from 7.4190 MPa to 10.0625 MPa). When *w=6 mm*, an increase of 36.48% in the compressive strength will be induced by an increase in the inclination angle from 0 to 90°. While θ=0°, if the flaw width increases from 2 to 6 mm, the compressive strength will decrease by 13.31%, and when θ=90°, a reduction of 12.76% in the compressive strength will be caused by the same rise in the flaw width. Based on these analyses, it can be concluded that an increase in the flaw width will increase the capability of the flaw inclination angle to increase the compressive strength, whereas a rise in the flaw inclination angle will decrease the ability of the flaw width to reduce the compressive strength. However, the difference obtained here is not very significant, and this means that the interaction between the flaw width and the inclination angle is not as strong as those between the flaw length and width, and the flaw length and the inclination angle.

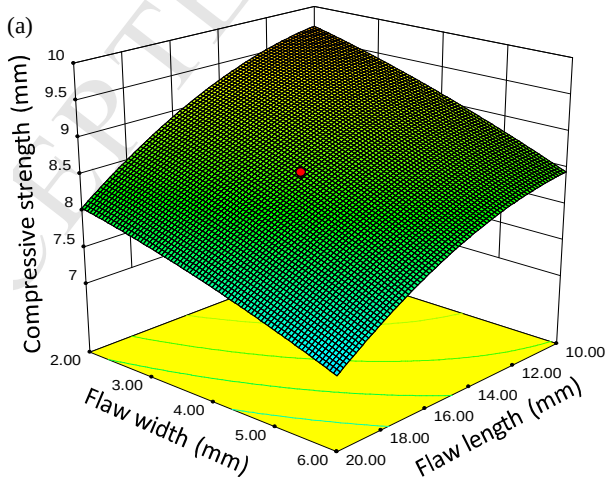

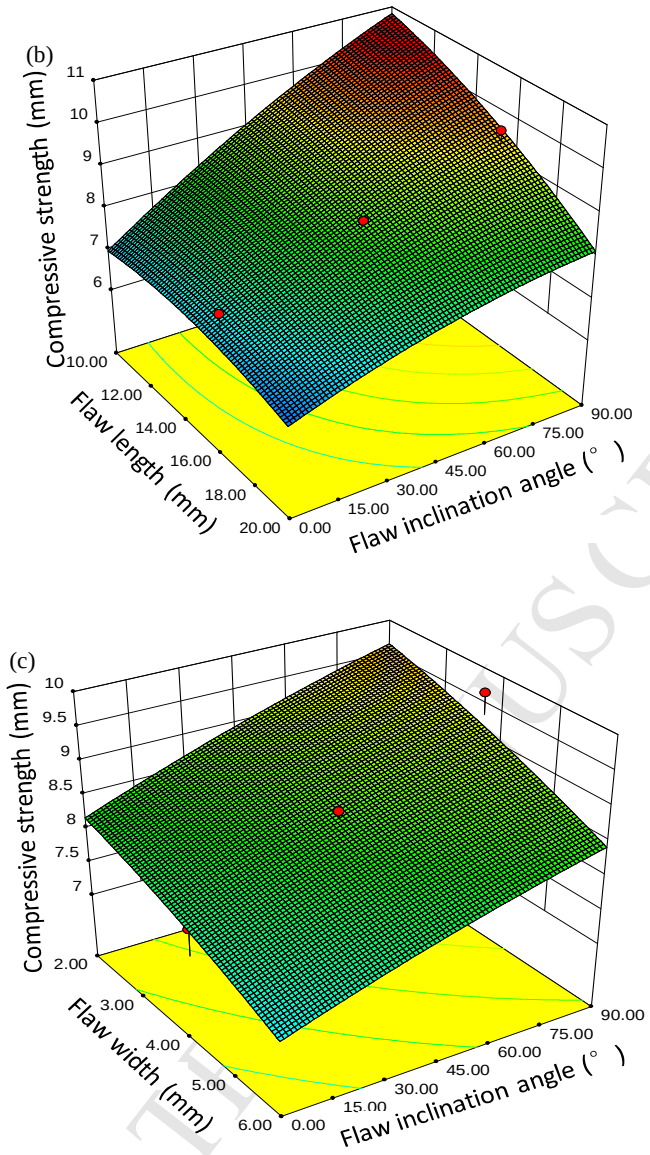

Fig.8. Response surface and contour plots that represent the effect of two variables and their interaction on the compressive strength of the precracked specimen when the other variable is at the middle level: (a) flaw length and flaw width; (b) flaw length and flaw inclination angle; (c) flaw width and flaw inclination angle.

4. Relationship between compressive strength and fractal dimension

In Section 3, the influences of the flaw parameters on the compressive strength were investigated using the control variate method and the central composite design method, and the variations of the compressive strength with the flaw parameters were discussed in detail. However, from Figs.3–5, it can be observed that the variations are not monotonous, and fluctuations are observed, i.e., the singular points marked with red ellipse. According to Zhao et al. (2015) and Yao et al. (2015), the mechanical properties of rock are closely related to crack propagation patterns. In addition, the effects of the flaw parameters can be ascribed to different crack propagation patterns. This means that different flaw parameters will result in various crack propagation patterns and thus, change the mechanical properties of the precracked specimen. Based on these analyses, further studies of crack propagation patterns are needed to have a better understanding of compressive strength.

It is well known that crack propagation pattern is a qualitative term. Because we want to obtain the relationship between the crack propagation pattern and compressive strength, it is necessary to identify the best way to quantify this term. Here, the fractal dimension is adopted to characterize the crack propagation pattern (Li et al., 2014). Fractal theory, which addresses the scaling of hierarchical and irregular systems, offers new opportunities for modeling the fragmentation process (Zhao, 1998). In this paper, the fractal dimension was adopted to characterize the evolution rules of the crack propagation trajectories. A smaller fractal dimension represents a simpler crack propagation trajectory, whereas a larger fractal dimension indicates a more complex crack propagation trajectory.

In the current work, the *Fractal Fox 2.0* software was used to calculate the fractal dimension based on the basic definition of the box dimension. The calculation results are depicted in Fig.9. The fractal dimension of a crack can be calculated according to Equation (6) (Li et al., 2014):

$$D = \log N(L) / \log(1/L) \tag{6}$$

where L is the side length of the square grid and $N(L)$ is the corresponding square grid number.

Here, the fractal dimension is the slope of the fitting line. The specific values are depicted in Figs.10(a)–(c).

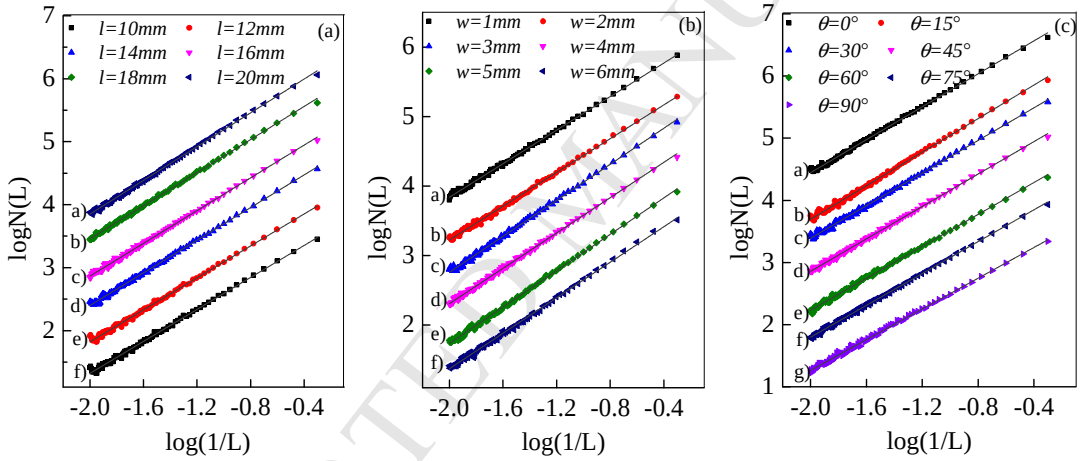

Fig.9. Plots of log$N(L)$ versus log$(1/L)$ of different flaw parameters: (a) flaw length; (b)flaw width; (c)flaw inclination angle. Successive lines are displaced by +0.5 units for clarity.

To determine how the crack propagation pattern affects the compressive strength, the crack of the specimen at the peak strength is displayed in Fig.10. The corresponding fractal dimension of the crack is also plotted. Note that the crack propagation patterns, fractal dimensions, and the compressive strengths used here are obtained from the first test (of the 3 total tests conducted).

Fig.10(a) presents the crack propagation patterns and the variations of the compressive strength and fractal dimension with the flaw length. With an increase in the flaw length, the compressive strength decreases gradually, whereas the fractal dimension shows the opposite trend. This is because an increase in the flaw length will result in a more complex crack propagation pattern, and more microcracks occur at the peak strength. This will lead to a lower compressive strength.

Fig.10(b) displays the crack propagation patterns, compressive strength, and fractal dimension with different flaw widths. With an increase in the flaw width, the compressive strength decreases with certain fluctuations. However, the fractal dimension shows an increasing trend, except for the points related to w=4 and 6 mm. The values of the compressive strength at these

points are higher than those around them, but their fractal dimensions are lower than those around them. This is because at these points, the crack propagation is more regular and fewer microcracks are formed compared with the points around them. This also indicates that a good relationship exists between the compressive strength and the fractal dimension.

The relationship between the compressive strength, fractal dimension, and the flaw inclination angle is depicted in Fig.10(c). A rise in the inclination angle leads to an increase in the compressive strength and a decrease in the fractal dimension, except at the 15° point. As in Figs.10(a) and 10(b), a good relationship between the compressive strength and the flaw inclination angle is also observed in Fig.10(c).

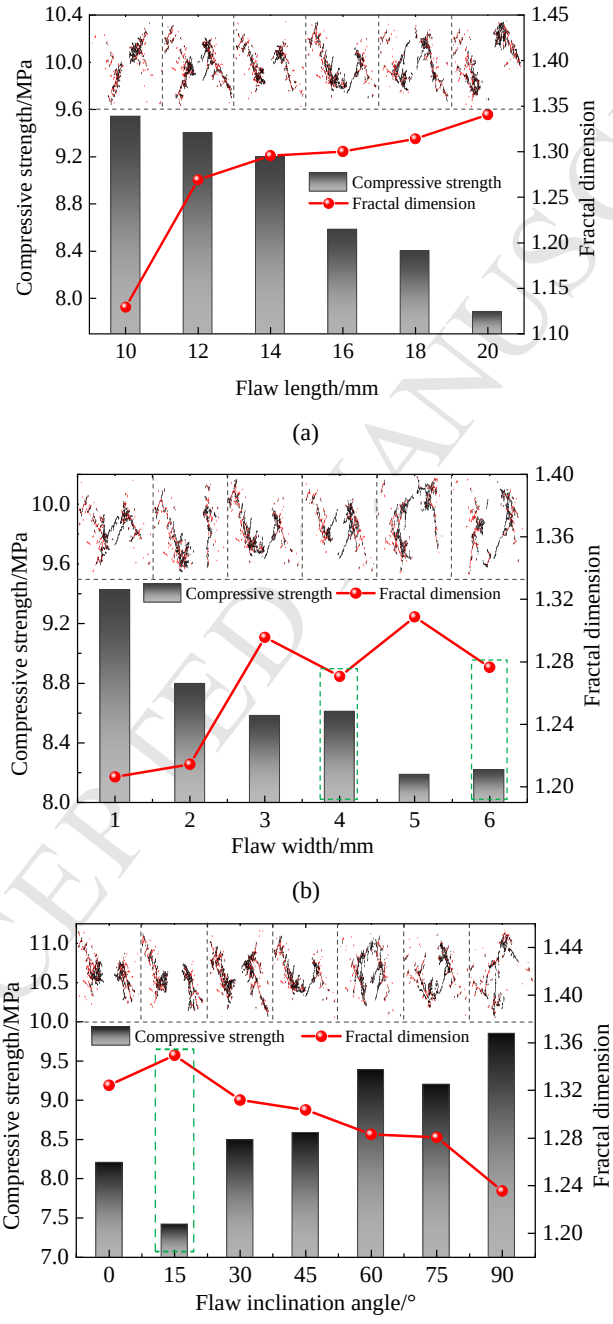

Fig.10. The relationship between the compressive strength, fractal dimension, and the flaw parameters: (a) flaw length; (b) flaw width; (c) flaw inclination angle.

ACCEPTED MANUSCRIPT

5. Guiding significance to field application of hydraulic slotting

In this work, the strength of the precracked specimen was chosen as the study index. If the specimen has lower strength, the coal mass breaks easily because lower strength favors the formation and propagation of cracks or fractures. In addition, more migration pathways for gas will become available, which will subsequently increase the gas drainage efficiency.

At present, the determination of flaw parameters for hydraulic slotting during field application lacks a theoretical basis. The results of this work demonstrate the influence of flaw parameters on hydraulic slotting. In addition, our results also indicate that there exists a coupled effect among the flaw parameters, which has a significant influence on the release of pressure and permeability enhancement effects of hydraulic slotting. The results of this research thus provide guidance and a theoretical basis to overcome the aforementioned limitation (i.e., obtaining flaw parameters for hydraulic slotting during field application).

6. Conclusions

A numerical model was constructed to investigate the compressive strength of coal after hydraulic slotting. A single flaw with different parameters (length, width, and inclination angle) was created at the center of the model. The influence of the flaw parameters on the compressive strength of a precracked specimen was studied using the response surface methodology and fractal method, and several meaningful conclusions have been drawn.

Using the control variate method, the effect of the single flaw on the compressive strength was investigated. The results show that with an increase in flaw length and width, the compressive strength decreases gradually, whereas an increase in the flaw inclination angle has a negative effect on the compressive strength.

The investigation of the influence of the coupled effect among flaw parameters on compressive strength indicates that an increase in the flaw width increases the capacity of the flaw length to weaken the compressive strength; in addition, an increase in the flaw length will also enhance the capacity of the flaw width to weaken the compressive strength. An increase in the flaw length will reduce the capability of the flaw inclination angle to enhance the compressive strength; and a larger flaw inclination angle, will increase the ability of the flaw length to reduce the compressive strength. An increase in the flaw width increases the capability of the flaw inclination angle to increase the compressive strength, whereas a rise in the flaw inclination angle will decrease the ability of the flaw width to reduce the compressive strength. The result of the analysis indicates that the interaction between the flaw width and the inclination angle is not as strong as that between the flaw length and the width or between the flaw length and the inclination angle.

The relationship between the compressive strength and the fractal dimension of the crack propagation pattern was also studied. The result implies that an opposite variation trend exists between the two parameters.

The results of the research indicate that the coupling effects of the flaw parameters have a significant influence on the compressive strength, and this effect should be considered during the design of the hydraulic slotting parameters before field application.

Acknowledgments

This work was supported by the State Key Basic Research Program of China (No.

2011CB201205), the National Natural Science Foundation of China (No. 51474211; 51204174; 51404261), the National Science and Technology Support Program (No. 2012BAK04B07), the Natural Science Foundation of Jiangsu Province (BK20140196), the Fundamental Research Funds for the central university (2014QNA02), and the China Postdoctoral Science Foundation funded project (2014M551057).

References

Chen, H.D., Jiang, J.Y., Chen, X.J., et al., 2014. Differences in coal bed methane occurrence for different regions of igneous erosion in the Haizi coal mine, Huaibei coalfield, China. Journal of Natural Gas Science and Engineering. 21, 732-737.

Cheng, Y.P., Wang, L., Zhang, X.L., et al., 2011. Environmental impact of coal mine methane emissions and responding strategies in China. International Journal of Greenhouse Gas Control. 5, 157-166.

Cho, N., Martin, C.D., Sego, D.C., 2007. A clumped particle model for rock. International Journal of Rock Mechanic and Mining Science. 44, 997–1010.

Hungerford, F., Ren, T., Aziz, N., 2013. Evolution and application of in-seam drilling for gas drainage. International Journal of Mining Science and Technology. 23, 543-553.

Kirmizakis, P., Tsamoutsoglou, C., Kayan, B., et al., 2014. Subcritical water treatment of landfill leachate: Application of response surface methodology. Journal of Environmental Management. 146, 9-15.

Lu, Y.Y., Liu, Y., Li, X.H., et al., 2010. A new method of drilling long boreholes in low permeability coal by improving its permeability. International Journal of Coal Geology. 84, 94-102.

Lu, T.K., Yu, H., Zhou, T.Y., et al., 2009. Improvement of methane drainage in high gassy coal seam using waterjet technique. International Journal of Coal Geology. 79, 40-48.

Lu, T.K., Zhao, Z.J., Hu, H.F., et al., 2011. Improving the gate road development rate and reducing outburst occurrences using the waterjet technique in high gas content outburst-prone soft coal seam. International Journal of Rock Mechanics & Mining Sciences. 48, 1271-1282.

Lin, B.Q, Liu, T., Zou, Q.L, et al., 2014. Crack propagation patterns and energy evolution rules of coal within slotting disturbed zone under various lateral pressure coefficients. Arabian Journal of Geosciences. doi: 10.1007/s12517-014-1728-9.

Lin, B.Q, Shen, C.M, 2015. Coal permeability-improving mechanism of multilevel slotting by water jet and application in coal mine gas extraction. Environment Erath Science. Doi: 10.1007/s12665-015-4154-8.

Lee, H., Jeon, S., 2011. An experimental and numerical study of fracture coalescence in pre-cracked specimens under uniaxial compression. International Journal of Solids and Structures. 48, 979-999.

Li, H.Q., Wong, L.N.Y., 2012. Influence of flaw inclination angle and loading condition on crack initiation and propagation. International Journal of Solids and Structures. 49, 2482-2499.

Li, D.J., Zhao, F., Mao, J., 2014. Fractal characteristics of cracks and fragments generated in unloading rockburst tests. International Journal of Mining Science and Technology. 24, 819-823.

Liu, H.B., Liu, H., Cheng, Y.P., 2014. The elimination of coal and gas outburst disasters by ultrathin protective seam drilling combined with stress-relief gas drainage in Xinggong coalfield. Journal of Natural Gas Science and Engineering. 21, 837-844.

Liu, T., Lin B.Q., Zou, Q.L., 2015. Investigation on mechanical properties and damage evolution of coal after hydraulic slotting. Journal of Natural Gas Science and Engineering. 24, 489-499.

Manouchehrian, A., Sharifzadeh, M., Marji, M., et al., 2014. A bonded particle model for analysis of the flaw orientation effect on crack propagation mechanism in brittle materials under compression. Archives of Civil and Mechanical Engineering. 14, 40-52.

Meng, J.Q., Nie, B.S., Zhao, B., 2015. Study on law of raw coal seepage during loading process at different gas pressures. International Journal of Mining Science and Technology. 25, 31-35.

Ni, G.H., Lin, B.Q., Zhai, C., et al., 2014. Kinetic characteristics of coal gas desorption based on the pulsating injection. International Journal of Mining Science and Technology. 24, 631-636.

Noshadi, I., Amin, N.A.S., Parnas, R.S., 2012. Continuous production of biodiesel from waste cooking oil in a reactive distillation column catalyzed by solid heteropolyacid: Optimization using response surface methodology (RSM). Fuel. 94, 156-164.

Park, C.H., Bobet, A., 2009. Crack coalescence in specimens with open and closed flaws: A comparison. International Journal of Rock Mechanics & Mining Sciences. 46, 819-829.

Paliwal, B., Ramesh, K.T., 2008. An interacting micro-crack damage model for failure of brittle materials under compression. Journal of the Mechanics and Physics of Solids. 56, 896-923.

Qin, Y.P., 2001. Discussion on damage mechanics model and constitutive equation of rock. Chinese Journal of Rock Mechanics and Engineering. 20, 560-562 (in Chinese).

Sodeifian,G.h., Azizi, J., Ghoreishi, S.M., 2014. Response surface optimization of SmyrniumcordifoliumBoiss (SCB) oil extraction via supercritical carbon dioxide. The Journal of Supercritical Fluids. 95, 1-7.

Shen, C.M., Lin, B.Q., Meng, F.W., et al., 2012a. Application of pressure relief and permeability increased by slotting a coal seam with a rotary type cutter working across rock layers. International Journal of Mining Science and Technology. 22, 533-538.

Shen, C.M., Lin, B.Q., Zhang, Q.Z., et al.,2012b. Induced drill-spray during hydraulic slotting of a coal seam and its influence on gas extraction. International Journal of Mining Science and Technology. 22, 785-791.

Shen, C.M., Lin, B.Q., Sun, C., et al., 2014. Analysis of the stress–permeability coupling property in water jet slotting coal and its impact on methane drainage. Journal of Petroleum Science and Engineering. http://dx.doi.org/10.1016/j.petrol.2014.11.035i.

Wong, R.H.C., Chau, K.T., 1998. Crack coalescence in a rock-like material containing two cracks. International Journal of Rock Mechanics & Mining Sciences. 35, 147-164.

Wong, L.N.Y., Einstein, H.H., 2009. Systematic evaluation of cracking behavior in specimens containing single flaws under uniaxial compression. International Journal of Rock Mechanics & Mining Sciences. 46, 239-249.

Wang, T., Zhou, W.B., Chen, J.H., et al., 2014. Simulation of hydraulic fracturing using particle flow method and application in a coal mine. International Journal of Coal Geology 121, 1-13.

Wang, L., Cheng, Y.P., 2012. Drainage and utilization of Chinese coal mine methane with a coal–methaneco-exploitation model: Analysis and projections. Resources Policy. 37, 315-327.

Wang, F.T., Ren, T., Tu, S.H., et al., 2012. Implementation of underground longhole directional drilling technology for greenhouse gas mitigation in Chinese coal mines. International Journal of Greenhouse Gas Control. 11, 290-303.

Xia, T.Q., Zhou, F.B., Liu, J.S., et al., 2014. A fully coupled coal deformation and compositional flow model for the control of the pre-mining coal seam gas extraction. International Journal of Rock Mechanics & Mining Sciences. 72, 138-148.

Yan, F.Z., Lin, B.Q., Zhu, C.J., et al., 2015. A novel ECBM extraction technology based on the integration of hydraulic slotting and hydraulic fracturing. Journal of Natural Gas Science and Engineering. 22, 571-579.

Yang, S.Q., Dai, Y.H., Han, L.J., et al., 2009. Experimental study on mechanical behavior of brittle marble samples containing different flaws under uniaxial compression. Engineering Fracture Mechanics. 76, 1833-1845.

Yang, S.Q., Jiang, Y.Z., Xu, W.Y., et al., 2008. Experimental investigation on strength and failure behavior of pre-cracked marble under conventional triaxial compression. International Journal of Solids and Structures.

ACCEPTED MANUSCRIPT

45, 4796-4819.

Yuan, Z.Y., Yang, J., Zhang, Y.F., et al., 2015. The optimization of air-breathing micro direct methanol fuel cell using response surface method. Energy. 80, 340-349.

Yao, Q.L., Li, X.H., Zhou, J., et al., 2015. Experimental study of strength characteristics of coal specimens after water intrusion. Arabian Journal of Geosciences. 10.1007/s12517-014-1764-5.

Yuan, X.P., Liu, H.Y., Wang, Z.Q., 2013. An interacting crack-mechanics based model for elastoplastic damage model of rock-like materials under compression. International Journal of Rock Mechanics & Mining Sciences. 58, 92-102.

Yang, W., Lin, B.Q., Wu, H.J., 2009. Study of the stress relief and gas drainage limitation of a drilling and the solving mechanism. Procedia Earth and Planetary Science. 1, 371-376.

Zhao, Y.H., 1998. Crack pattern evolution and a fractal damage constitutive model for rock. International Journal of Rock Mechanics & Mining Sciences. 35, 349-366.

Zhang, X.P., Wong, L.N.Y., 2012. Cracking process in rock-like material containing a single flaw under uniaxial compression: a numerical study based on parallel bonded-particle model approach. Rock Mech Rock Eng. 45, 711-737.

Zhang, X.P., Wong, L.N.Y., 2013a. Crack initiation, propagation and coalescence in rock-like material containing two flaws: a numerical study based on bonded-particle model approach. Rock Mech Rock Eng. 46, 1001-1021.

Zhang, X.P., Wong, L.N.Y., 2013b. Loading rate effects on cracking behavior of flaw-contained specimens under uniaxial compression. Int J Fract. 180, 93-110.

Zhang, H.R., Pera, L.S., Zhao, Y.J., et al., 2015. Researches and applications on geostatistical simulation and laboratory modeling of mine ventilation network and gas drainage zone. Process Safety and Environmental Protection. 94, 55-64.

Zhang, B., Chen, G.Q., Li, J.S., et al., 2014. Methane emissions of energy activities in China 1980–2007. Renewable and Sustainable Energy Reviews. 29, 11-21.

Zhou, J.W., Xu, W.Y., Yang, X.G., 2010. A microcrack damage model for brittle rocks under uniaxial compression. Mechanics Research Communications. 37, 399-405.

Zhou, H.X., Yang, Q.L., Cheng, Y.P., et al., 2014. Methane drainage and utilization in coal mines with strong coal and gas outburst dangers: A case study in Luling mine, China. Journal of Natural Gas Science and Engineering. 20, 357-365.

Zhou, H.X., Zhang, R., Cheng, Y.P., et al., 2015. Methane and coal exploitation strategy of highly outburst-prone coal seam configurations. Journal of Natural Gas Science and Engineering. 23, 63-69.

Zou, Q.L., Lin, B.Q., Liu, T., et al., 2014a. Variation of methane adsorption property of coal after the treatment of hydraulic slotting and methane pre-drainage: A case study. Journal of Natural Gas Science and Engineering. 20, 396-406.

Zou, Q.L., Lin, B.Q., Liang, J.Y., et al., 2014b. Variation in the pore structure of coal after hydraulic slotting and gas drainage. Adsorption Science & Technology. 32, 647-666.

ACCEPTED MANUSCRIPT

1. Influences of single parameters of flaw on the compressive strength of precracked specimen are studied using control variate method.
2. Effects of interactions among flaw parameters on the compressive strength of precracked specimen are investigated by response surface methodology (RSM).
3. Crack propagation patterns of precracked specimen are quantified by fractal method.
4. Relationships between the compressive strength and fractal dimension are discussed.

ACCEPTED MANUSCRIPT